Journal of Thermal Analysis and Calorimetry (2024) 149:6039–6050
https://doi.org/10.1007/s10973-024-13208-2

Thermal decomposition study of carbon fiber-reinforced polyphenylene sulfide at high heating rates met under fire exposure

Yann Carpier[1] · Aurélie Bourdet[2] · Nicolas Delpouve[2] · Éric Dargent[2] · Benoit Vieille[1]

Received: 27 October 2023 / Accepted: 9 April 2024 / Published online: 2 May 2024

Abstract

Performing pyrolysis studies on polymer matrix composites, at rates that match the elevation of temperature met during a fire exposure, is of primary interest for the aeronautics field. In this study, one aspect of the material response under flame is investigated, which is the thermal degradation of the polymer matrix. Thermogravimetric analyses (TGA), up to five hundred Kelvins per minute, are performed on polyphenylene sulfide (PPS) and carbon fiber-reinforced polyphenylene sulfide (CF/PPS), to mimic the heating rate conditions commonly met during a fire. The influence of the heating rate regarding the PPS decomposition signature is discussed from both the residual mass and the characteristic temperature corresponding to the maximum rate of degradation. Then, the PPS thermal decomposition features are compared with those of several thermoplastic polymers and thermoplastic–based composites. It is observed that PPS stands out when subjected to fast elevation of temperature. Indeed, its amount of «char», obtained after thermal degradation, increases with the heating rate. To investigate possible mechanistic causes behind this singular behavior, the influence of the heating rate on the degradation mechanisms occurring into PPS and CF/PPS is investigated. TGA coupled with Fourier transform infrared spectroscopy (FTIR) is used to obtain the decomposition products. The results plaid for the coexistence of two main degradation mechanisms, being the random chain–scission and the depolymerization. Nevertheless, when the heating rate increases, the random chain–scission seemingly becomes the predominant mechanism along the whole process.

✉ Nicolas Delpouve
nicolas.delpouve1@univ-rouen.fr

[1] Groupe de Physique des Matériaux, CNRS, INSA Rouen Normandie, UMR 6634, 76000 Rouen, France

[2] Groupe de Physique des Matériaux, CNRS, Univ Rouen Normandie, UMR 6634, 76000 Rouen, France

Graphical abstract

Keywords Thermogravimetric analysis · Composites · PPS · Pyrolysis

Introduction

Since several years, the properties of composites exposed to fire have been extensively investigated [1–8]. The demand in polymer-based composites is growing in aeronautics and aerospace engineering, as they have high strength over density ratio. Thermosetting matrixes have been widely used for fifty years, but recently, the number of studies regarding thermoplastics, notably polyphenylene sulfide (PPS) or polyether ether ketone (PEEK), has increased [9–15]. Thermoplastic–based composites offer indeed some advantages for industrial applications, notably their ease in manufacturing [16]. In addition, they show better damage tolerance and impact resistance [17]. Safety reasons in aircraft naturally lead to investigate the thermal resistance of these composites, as well as the mechanisms of decomposition and the sub-products generated during fire propagation. Besides, the mechanism of fire-extinguishing agents is commonly investigated through observation of the thermal decomposition process [18].

The response of a thermoplastic composite exposed to a flame can be perceived as the conjunction of several phenomena impacting macroscopic properties [19], among which the diffusion of heat by conduction, generating physical and chemical transformations through the thickness of the material [20], the creation of porosities linked to the formation of gas bubbles within, and the release of pyrolysis gases that could feed the fire [21]. Moreover, the nature of the response depends on both the flame properties and the environing atmosphere, which forces to consider multiple scenarios. Investigating these phenomena individually offers an opportunity to understand their action before they manifest together. Our study focuses on pure thermal degradation, by opposition to the thermally–oxidative one, which exhibits its own peculiarities. The thermal decomposition of carbon fiber reinforced PPS composite (CF/PPS) is investigated for heating conditions matching those encountered during fire. This material is well representative of thermoplastic composites for aeronautics applications since carbon fibers are usual reinforcements to polymer matrixes, which exhibit high thermal resistance under inert atmosphere, their sublimation temperature being above 3000 °C [22].

The thermal degradation of polymers is a complex process that may involve several chemical reactions, sometimes concomitant, such as random–chain scission, end-chain scission, cross-linking [23] among others. Thermogravimetric analysis has widely been used to depict the thermal decomposition of a material as it allows correlating mass

loss with temperature or time [24]. Coupling thermal analysis with mass spectroscopy (MS) improves the knowledge regarding the degradation mechanisms. The non-isothermal decomposition of PPS has already been investigated from direct pyrolysis-mass spectrometry (Py–MS) [25], flash pyrolysis–gas chromatography/mass spectrometry (Py–GC/MS) [26], stepwise pyrolysis–gas chromatography/mass spectrometry (stepwise Py–GC/MS), and by TGA–mass spectrometry (TGA–MS) techniques [27]. Although the mechanism chronology is not perfectly established, the decomposition of PPS can be described as a competition between depolymerization and random chain scission, respectively, leading to the formation of thiophenol on one side, and of benzene and hydrogen sulfide on the other side [27, 28]. The coupling of TGA with Fourier transform infrared spectroscopy (TGA–FTIR) is a complementary tool to study thermal degradation mechanisms. The volatile compounds are analyzed in isothermal or non–isothermal conditions, the knowledge of their respective amount being useful for the representation of the successive steps of decomposition. Di et al. used TGA–FTIR to show that the melamine addition to an ethylene–vinyl acetate copolymer improves the flame retardancy because the thermal decomposition of melamine produces a substantial amount of non-flammable gases [29]. TGA–FTIR has also been proposed to study flame retardancy in polycarbonate and poly (vinyl chloride) [30, 31]. Regarding degradation mechanisms, the thermal decomposition of PPS has also been investigated by TGA–FTIR. The formation of thiophenol has thus been evidenced by Erickson [32], in consistence with TGA–MS results [27].

By exposing CF/PPS laminates to a heat flux of 50 kW/m^2, Carpier et al. [33] have shown that the temperature of the composite rises quickly, the heating rate approaching 150 K min^{-1} on the back face, and exceeding 400 K min^{-1} on the exposed face. Unfortunately, these heating conditions, reproducing a fire of medium intensity, are rarely mimicked when performing TGA investigations, which might call into question the relevance of TGA to investigate the behavior of composite exposed to fire [23]. Consequently, the fields for which fire safety is at stake, including aeronautics, could benefit from high-rate TGA investigations. However, performing experiments at such rates is not an easy task. Indeed, by increasing the heating rate, the interpretation of the results becomes more uncertain due to thermal conductivity issues. Vanden Poel et al., using differential scanning calorimetry, reported that both mass and heating rate influence the thermal lag [34]. When the sample mass increases, the thermal lag between the sample temperature and the sensor temperature also increases. When the heating rate increases, the sensor temperature shifts with respect to the furnace temperature. Thus, the planification of such measurements implies to consider how the observables commonly deduced from TGA investigations, particularly the characteristic temperatures, are impacted by the increase in the heating rate.

The purpose of this study is to bring new results regarding the non–isothermal thermal decomposition of PPS and CF/PPS, by carrying analyses under nitrogen atmosphere at high rates, up to 500 K min^{-1}, corresponding to those encountered during a fire. The first part of the study evaluates the feasibility and the limitations of high-rate TGA by following the response of a standard of nickel used for calibration under various heating rates. The second part of this study is dedicated to the singularities of the TGA responses obtained at high-rate, by confronting the results obtained from the investigations on PPS to the response of several polymers. Finally, the non-isothermal decomposition mechanisms of PPS and CF/PPS are studied by TGA–FTIR under nitrogen.

Experimental

Materials

Poly (phenylene sulfide) (PPS) Fortron 0214 Celanese® grade was purchased by Ticona®. The carbon reinforcement is a balanced fabric with a pattern of 5-harness satin weave (T300 3K 5HS, Toray). The volume fraction of fibers is 50% which corresponds to a matrix mass content of 42%. The composites design consists in 7-ply laminates with an angle ply $\{\pm 45\}7$ stacking sequence [35]. To better singularize the heating rate dependence of the PPS decomposition from others, TGA experiments were performed on several polymers with diversified chemical structure. EcoPaXX® PA 410 was obtained from DSM®, PET samples were obtained from 500 µm thick films extruded by Carolex Co. ® (The number–average molecular weight is: Mn = 31000 g mol^1), PLA grade was 4042D with a D content of 4% as provided by NatureWorks®, PE and PA6 industrial grades were generously given by Shell France®.

Instruments

The TGA experiments were performed in platinum pans compatible with high temperature, from 25 to 700 °C, in a Thermal Analysis® Discovery apparatus, under a nitrogen dynamic gas flow of 25 mL min^{-1}, with a balance purge of nitrogen at 25 mL min^{-1}. The sample mass was ranging between 0.5 and 2 mg. Conventional to high heating rates were used, i.e., 10, 20, 50, 100, 200, 400, and 500 K min^{-1}. The calibration in mass was done by using mass standards and a verification of the mass loss was performed with calcium oxalate. The calibration in temperature used the Curie point of nickel. Its detection dependence to the heating rate is provided in the following section.

The decomposition products were analyzed for several rates thanks to the TGA–FTIR coupling by connecting a transfer line between the Thermal Analysis® Discovery apparatus and a NicoletTM iSTM10 FT–IR spectrometer from Thermoscientific®, equipped with a Helium–Neon laser source, a Ge/KBr beam splitter, and a deuterated triglycine sulfate (DTGS) pyroelectric detector. The spectra were interpreted with the help of the OMNIC® series acquisition software. To improve the detection of the decomposition products, especially for CF/PPS, the sample mass was situationally increased up to 15 mg.

Results and discussion

Pre-experimental tests at high rates

Classically, any TGA set of experiments is preceded by a calibration in temperature, which is performed by analyzing a standard for which the temperature of Curie is known. This corresponds to the temperature at which a magnetic compound loses its permanent magnetic properties, thus transiting from ferromagnetic or ferrimagnetic to paramagnetic. The reduced attraction for the magnet results in a sharp apparent mass loss or gain [36]. Sharp Curie points, identified by thermal analysis [37], are used to generate a very high accuracy temperature correction curve [38, 39]. Fig. 1 presents the typical result we obtain from the analysis of nickel at the rate of 20 K min^{-1} that is used for the temperature calibration of the apparatus, according to the manufacturer recommendation. One can observe first an apparent increase of the mass at the equilibration temperature which results from the attraction of the magnetic sample to the magnet. This attraction vanishes at the temperature of Curie (i.e., $T_{Endset1}$ = 361.49 °C there), leading to the apparent mass loss. Then, the obtained value $T_{Endset1}$ is confronted to the literature reference of the Curie point of nickel ($T_{Curieref}$ = 356.86 °C), and a correction is established for all experiments following this calibration.

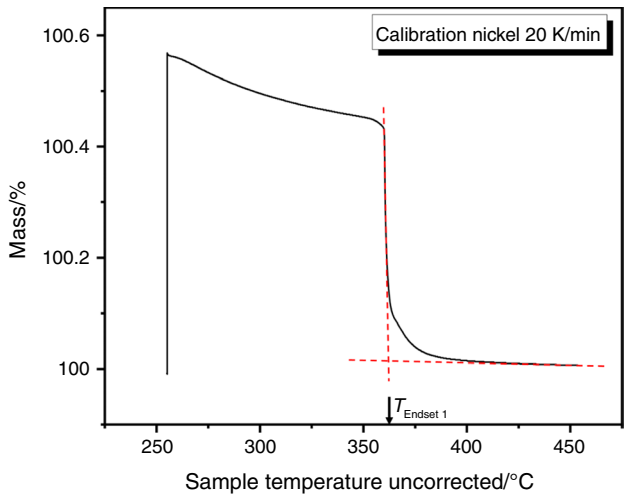

Fig. 1 Curie point determination for nickel with a heating rate of 20 K min^{-1}. The calibration is performed under nitrogen atmosphere

Then, a control experiment has been performed at 20 K min^{-1} to evaluate the accuracy of the correction associated with the calibration. The second run at 20 K min^{-1} (presented in Fig. 2a) provides the value $T_{Endset2}$ = 356.83 °C, which is 5 °C lower than $T_{Endset1}$, and can be considered equivalent to $T_{Curieref}$ = 356.86 °C, as one can expect from a successful calibration. When the heating rate ranges from 5 to 50 K min^{-1}, the analysis of nickel leads to similar results, that is $T_{Endset} \cong T_{Curieref}$ = 356.83 °C. This confirms the efficiency of the post–calibration correction in this interval. Nevertheless, at 100 K min^{-1} and beyond, the

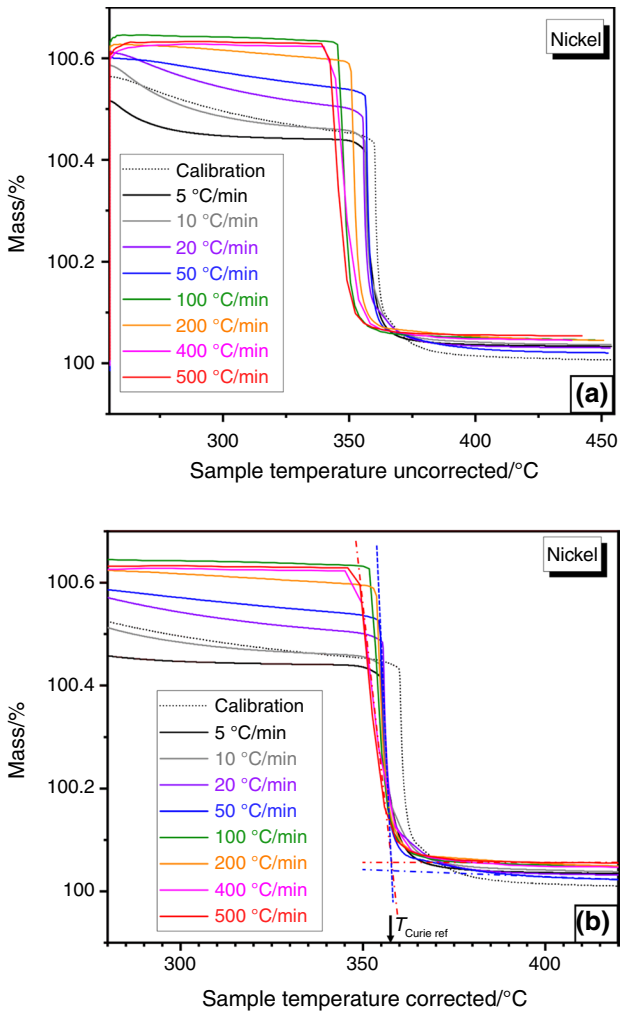

Fig. 2 TGA experiment performed under nitrogen on a nickel sample at various heating rates following the calibration in temperature performed at 20 K min^{-1}: **a** without further correction, **b** after correcting the heating rate dependence of the nickel TGA response

Curie transition is detected at lower temperature (Fig. 2a). Moreover, it appears broadened, especially at 400 and 500 K min^{-1}. At 500 K min^{-1}, the experimental T_{Endset} divergence from T_{Curieref} is close to 10 °C. Such gap certainly impacts all measurements performed at high rates. The curves obtained after correction of this shift are presented in Fig. 2b.

Heating rate dependence of the PPS decomposition signature

We now focus on the analysis of PPS thermal degradation. To assess that the experimental procedure is followed during the TGA run, the sensor temperatures are plotted versus time in Fig. 3. Sensor temperatures almost instantaneously align with the theoretical time/temperature dependence at 5, 10 and 20 K min^{-1}, while at 50 K min^{-1} and beyond, a delay time is needed for the sensor temperature (solid line) to adjust to the program temperature, which duration ranges between 2 and 6 s, with no clear tendency regarding its evolution with the heating rate. Slight deviations from the heating program are occasionally observed, at 50 and 500 K min^{-1} for example, but they remain relatively marginal. At the chosen rates, the sensor temperature always follows the program starting from 50 °C, i.e., far before the onset of the PPS degradation. Thus, the experimental conditions are acceptable to investigate the PPS pyrolysis.

TGA results, consecutive to the analyses of PPS at various rates, are presented in Fig. 4. For the sake of clarity, the curves have been reported separately. Fig. 4a shows that the signature of PPS degradation shifts toward higher temperatures when the heating rate increases from 5 to 200 K min^{-1},

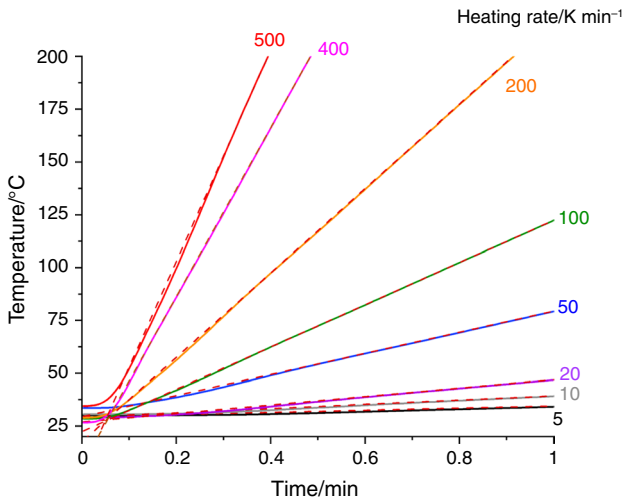

Fig. 3 Sensor (solid lines) versus time during the TGA scans of PPS performed under nitrogen atmosphere at several heating rates: 5; 10; 20; 50; 100; 200; 400 and 500 K min^{-1}. Theoretical time/temperature dependence for each rate is indicated by dashed lines

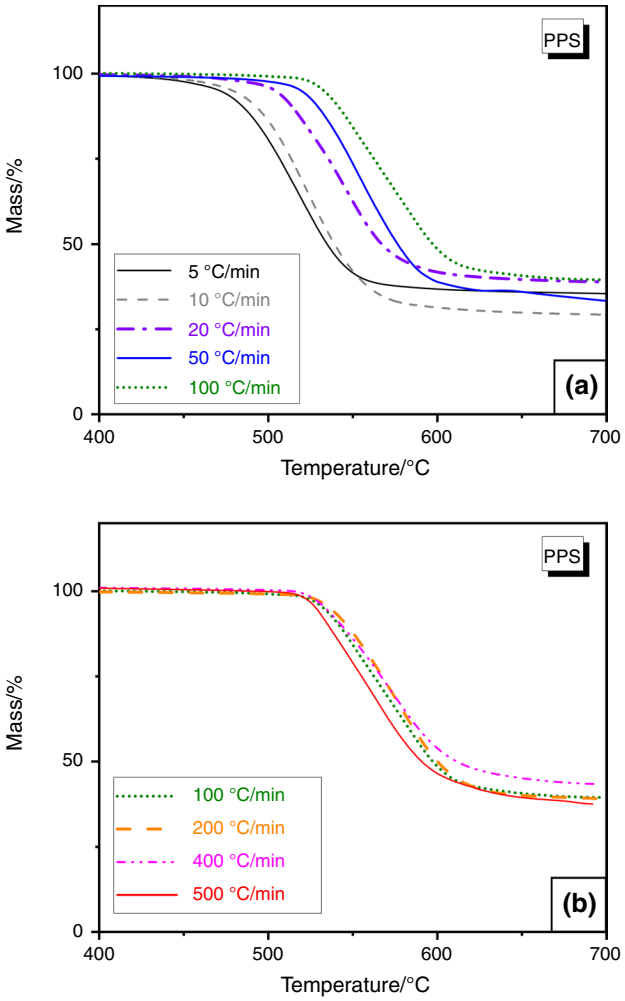

Fig. 4 TGA experiment performed under nitrogen on a PPS sample at various heating rates: **a** 5; 10; 20; 50; and 100 K min^{-1} **b** 100; 200; 400 and 500 K min^{-1}

whereas Fig. 4b shows the reverse tendency when the heating rate continues increasing from 200 to 500 K min^{-1}.

To investigate whether this heating rate dependence of the degradation signature relates to the PPS, or is a consequence of the experimental procedure itself, the same experiment has been repeated on several polymers, including some which do not share similarities with PPS in their chemical structure (experimental curves given in Fig. SI.1 of supporting information). Similar trends were observed independently on the polymer chosen. Fig. 5a gives the shift of the degradation signature as a function of the heating rate for HDPE, PET, EcoPaXX, PLA, PA6, and PPS. This shift corresponds to the difference between $T_{\text{d max}}$ the rate dependent temperature at which the decomposition is the fastest, and $T_{\text{d (5 K min}^{-1})}$ which corresponds to the reference temperature at which the decomposition is the fastest when the heating rate is equal to 5 K min^{-1}. Let us recall that $T_{\text{d max}}$ does not necessarily correspond to the half of process. For

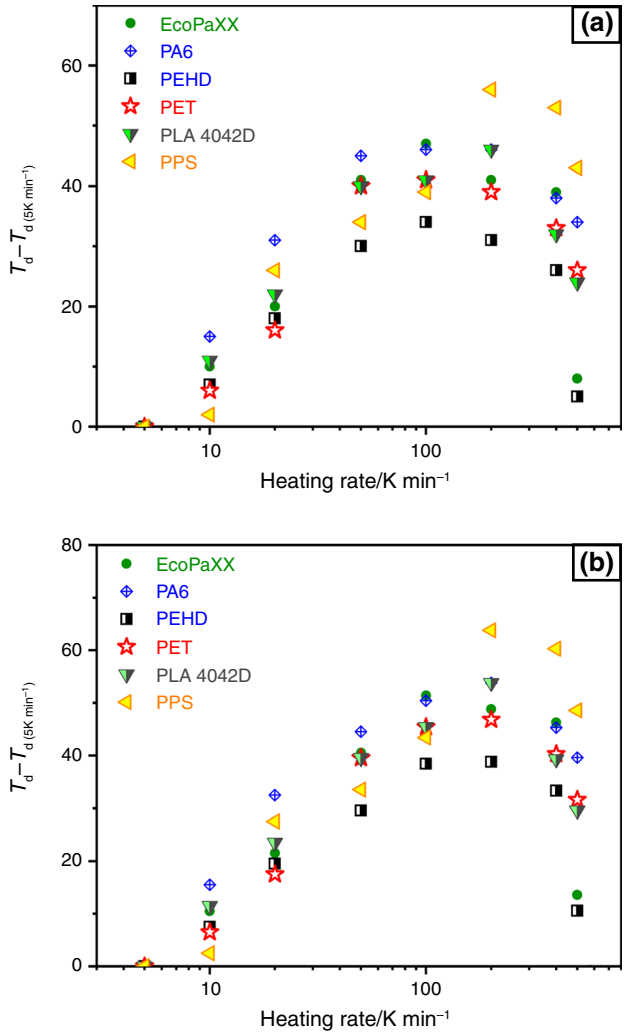

Fig. 5 Shift of the degradation signature $T_{d\,max}$–$T_{d\,(5\ K\ min^{-1})}$ as a function of the heating rate for HDPE, PET, EcoPaXX, PLA, PA6, and PPS. $T_{d\,max}$ is the rate dependent temperature at which the decomposition is the fastest. $T_{d\,(5\ K\ min^{-1})}$ corresponds to the reference temperature at which the decomposition rate is the fastest when the heating rate is equal to 5 K min^{-1}. The TGA investigations were performed at the following heating rates: 5; 10; 20; 50; 100; 200; 400 and 500 K min^{-1}: **a** without further correction, **b** after correcting the heating rate dependence of the nickel TGA response

this reason, slight discrepancies may be found regarding the data plotted on Fig. 5a with respect to the visual impression let by the curves of Fig. 4 and Fig. SI.1. Nevertheless, the profiles obtained in Fig. 5a highlight unambiguously that independently on the polymer chemical structure, the profile of $T_{d\,max}$–$T_{d\,(5\ K\ min^{-1})}$ vs. the heating rate is the same.

From 10 to 100 K min^{-1}, the data seem to align on the same trend, with $T_{d\,max}$–$T_{d\,(5\ K\ min^{-1})}$ progressively increasing with the heating rate. The rate of 200 K min^{-1} marks the maximum of $T_{d\,max}$–$T_{d\,(5\ K\ min^{-1})}$ that precludes a drop at higher rates. Interestingly, the decrease in a characteristic temperature at the highest heating rates is also reported in the case of the Curie temperature of nickel (Fig. 2a). On the other hand, when the heating rate ranges between 5 and 50 K min^{-1}, the Curie temperature detection is independent on the heating rate, whereas the polymer decomposition signature shifts toward higher temperatures. Therefore, we assume that the profile observed in Fig. 5a results from the combination of two effects.

The first effect would be linked to lags between both furnace and sensor temperatures [34], causing the TGA signature to shift toward low temperatures at high heating rates. By applying on this set the same correction that was performed after the analysis of nickel to obtain Fig. 2b, Fig. 5b is obtained, showing no real change regarding the obtained profile. This suggests that this effect could be sample dependent, maybe not reproducible regarding its amplitude. It is worth mentioning that performing the same correction for other characteristic temperatures, e.g., the temperature corresponding to 95% of mass loss, will lead to the same observations. It will be interesting to investigate how the instrument adapts to the temperature program and what are the consequences in terms of thermal lag within the furnace. The second effect would be linked to the thermal conductivity of the sample, increasing the thermal lag between the sample temperature and the sensor temperature, so causing the TGA signature to shift continuously toward high temperatures when increasing the heating rates. It was previously reported by Vanden Poel et al. [34] as mass effect.

The thermal conductivity impact on the TGA response can be highlighted by performing several runs at the same rate with varying the sample mass. Fig. 6 shows the curves obtained from the analyses of PPS samples of 0.2, 0.8, and 2 mg at 10 K min^{-1} (Fig. 6a), 50 K min^{-1} (Fig. 6b) and 500 K min^{-1} (Fig. 6c). To compare the behavior of PPS with other systems, the responses of PLA and HDPE of identical mass are added. For all systems, the signature of the degradation is recorded at slightly higher temperatures when the sample mass increases. This shift remains subtle among the selected sample masses. To magnify the thermal lag, a PLA sample of 20 mg has been analyzed at 500 K min^{-1}. We observe that increasing the mass of PLA sample by two decades (from 0.2 to 20 mg) shifts the degradation signature toward higher temperatures, about 90 K at the half of the decomposition.

Looking at the influence of the heating rate on the residual mass for samples with similar initial mass (Fig. 6), the thermal degradation leads or not to the full decomposition of the sample, depending on the polymer investigated. In some polymers, e.g., thermally stable polymers exhibiting aromatic cycles, such as PPS and PEEK [40], the pyrolysis leads to the formation of a carbon mass residue, named «char», that slowly decomposes with temperature. Char is a highly porous material that can consist of crystalline, i.e., graphitic, and/or amorphous regions, with the relative

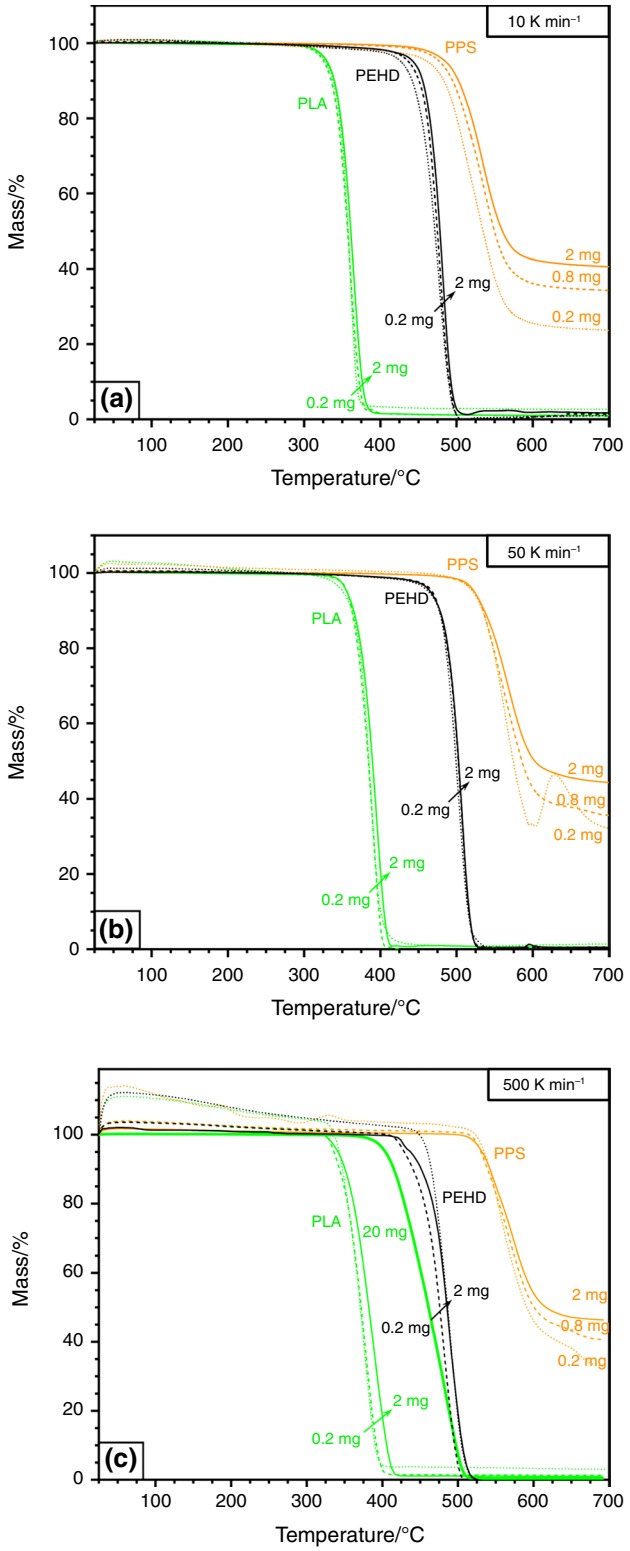

Fig. 6 Influence of the sample mass on the degradation signature of three polymers: PLA, PEHD and PPS for a heating rate of **a** 10 K min^{-1}, **b** 50 K $min^{-1}$and **c** 500 K min^{-1}

amounts of these phases determined by the original chemical composition of the polymer, as well as the temperature and testing atmosphere [41]. The char formation consumes energy and slows down the degradation. Moreover, when it is formed at the material surface, the char might favor the flame retardation [42, 43].

The composition and structure of char have been studied by Levchik et al [40]. It consists mostly of carbon (~ 85–98%) with trace amounts of aromatic–aliphatic compounds often with heteroatoms (O, N, P, S). The amount of char formed in a composite material is dependent on the chemical nature of both the polymer matrix and the organic fibers. Depending on the chemical processes governing the thermal decomposition, polymers can be categorized into three classes [40]. The thermal degradation of the first class is characterized by random chain scission reactions in which almost all the molecular structure becomes fragmented into volatile gases, resulting in a negligible amount of char. Polyolefin thermoplastics (e.g., polypropylene, polyethylene) situate among this class with other thermoplastics such as polystyrene (PS) and polymethyl methacrylate (PMMA). The second group undergoes random chain scission, end-chain scission, and chain stripping reactions, which leads to the loss of hydrogen atoms, pendant groups, and other low molecular mass organic groups from the main chain. These polymers yield a small amount of char, typically 5–20% of the original mass, and they include notably epoxies and polyvinyl chlorides (PVC). The third group structure features a high aromatic ring content that decomposes into aromatic fragments that fuse via condensation reactions to produce moderate to high amounts of char. Aromatic rings are the basic building blocks from which char is formed, and therefore the higher the aromatic content of the polymer the higher the char yield [44]. In the case of PPS, char results from cyclization reactions, occurring between different decomposition products [25]. Generally, high–performance thermostable thermoplastics (e.g., PPS, PEEK) yield high amounts of char (typically 30–40%). Thermogravimetric analyses (TGA) experiments performed on PEEK at 10 K min^{-1} revealed that under neutral atmosphere, the char slowly decomposes after its formation (about 12% of polymer initial mass, i.e., 30% of the char, from 600 °C to 900 °C) [12, 45].

As shown in Fig. 6a, the residual mass percentage of a 2 mg PPS analyzed at 10 K min^{-1} is 40% at 700 °C. This result is consistent with previous TGA investigations at 10 K min^{-1} leading to 45% residue from an about 10 mg PPS sample [33]. This confirmed the thermostable character of PPS, yielding to significant amount of char. Post–TGA microscopic observations, revealed that the char takes the form of a bubble resulting from the swelling of the material under high internal pressure. In carbon fiber-reinforced PPS (CF/PPS), consisting of 43% by mass of PPS, pyrolysis

under nitrogen at 10 K min^{-1} only resulted in a mass loss of 26% at 900 °C, with a maximum decomposition rate at 550 °C [33].

By increasing the heating rate, the char amount resulting from PPS thermal decomposition also increases. It is equal to 45% when the TGA rate is 50 K min^{-1} (Fig. 6b), and to 47% when the TGA rate is 500 K min^{-1} (Fig. 6c). The cross comparison between figures leads to similar observations independently on the sample mass. The residual mass percentage of a 0.8 mg PPS analyzed at 10 K min^{-1} is 34% at 700 °C, while it is equal to 35% when the TGA rate is 50 K min^{-1}, and to 40% when the TGA rate is 500 K min^{-1}. Finally, a 0.2 mg PPS analyzed at 10 K min^{-1} has a residual mass percentage of 24% at 700 °C but more than 30% when it analyzed at 500 K min^{-1}. The analysis at 50 K min^{-1}, which shows perturbations around 600 °C, also leads to more than 30% residual mass. We note that the analyses performed at 500 K min^{-1} on 0.2 mg samples are characterized by uncertainties regarding the mass measurement during the first seconds, independently on the polymer, due to imperfect equilibration. The time needed for the balance to compensate the disequilibrium is close to the time window preceding the decomposition. Imperfect equilibration is certainly detrimental for quantitative interpretations. Even if removing this set of data, the amount of the PPS char still increases with the heating rate.

The formation of a char layer in composite laminates is an important process because it can promote significant flame retardation [42, 43]. Therefore, the aptitude of PPS to generate higher char content when heated at high rates is of interest. On the other hand, one can also wonder whether this behavior is specific to PPS or shared by all thermostable polymers. In Fig. 7, the results obtained for PPS are compared with those obtained from previous studies regarding other «char–forming» materials: PEKK, PEKK mixed with a flame retardant [46], and a hybrid quasi–isotropic composite laminate consisting of carbon/glass fibers and a PEEK thermoplastic matrix (CG/PEEK) [47]. For these three systems a decrease in the residual mass percentage is observed when increasing the heating rate. PPS singularizes from all these systems by being the only one for which a lesser amount of material decomposes when increasing the heating rate. The heating rate influence on the TGA signature of CF/PPS is showed in supporting information (Fig. SI.2). CF/PPS behavior is essentially like PPS one. Indeed, both dependences on the heating rate, i.e., the degradation signature and the residual mass percentage, are following the same trend.

It is worth reminding that the char acts as a barrier to inhibit gaseous products from diffusing to the flame and shield the polymer surface from heat and air. It insulates the material from flame and prevents the volatile combustible gases from exiting the bulk. Many phosphorous-based flame retardants are added to composites owing to their ability to promote the formation of char [48]. Obviously, the structural integrity of polymer matrix composites is more likely to be preserved when the amount of char is maximized, which, according to several sources [49, 50], is connected to the decrease in the heating rate. The results obtained for PEEK and PEKK materials are consistent with these reports; however, PPS and CF/PPS seem to behave differently. This intriguing feature may be related to mechanistic differences depending on the heating rate. Since a change in decomposition mechanism could be revealed by the nature of the formed chemicals, PPS and CF/PPS gases from pyrolysis have been analyzed using TGA–FTIR.

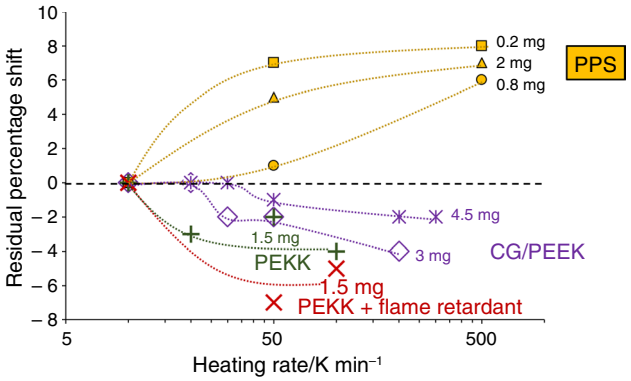

Fig. 7 Shift of the TGA residual mass percentage measured at 700 °C and at several heating rates, ranging from 10 to 500 K min^{-1}, for various «char–forming» materials: PPS (0.2, 0.8 and 2 mg samples), PEKK (1.5 mg samples), PEKK mixed with a flame retardant (1.5 mg samples), and CG/PEEK (3 mg and 4.5 mg samples). The residual mass at 10 K min^{-1} is set as the reference value, thus the value of the shift is equal to zero for all materials at 10 K min^{-1}. The dashed line indicates the hypothetic case for which the residual mass is invariant with the heating rate. Dotted lines are guidance for the eyes

Analysis of the PPS and CF/PPS decomposition gases by TGA–FTIR

In Fig. 8 are presented the results obtained from TGA–FTIR investigations on PPS at 50 K min^{-1}. The Gram–Schmidt signal provides, for a given time, the sum of the entire IR absorbance for all wavenumbers. It defines the interval during which the gases from thermal decomposition are detected. Its maximum is related to the maximum rate of the degradation. At regular intervals of the decomposition process, i.e., at different areas of the Gram–Schmidt signal, an infrared spectrum is recorded. Thus, the decomposition gases are continuously analyzed and it is possible to catch the infrared spectrum obtained at the very beginning of the decomposition, at the end, or when the process reaches its maximum rate. For each probed area of the Gram–Schmidt signal, the agreement between the infrared spectrum resulting from the analysis of the decomposition gases and the

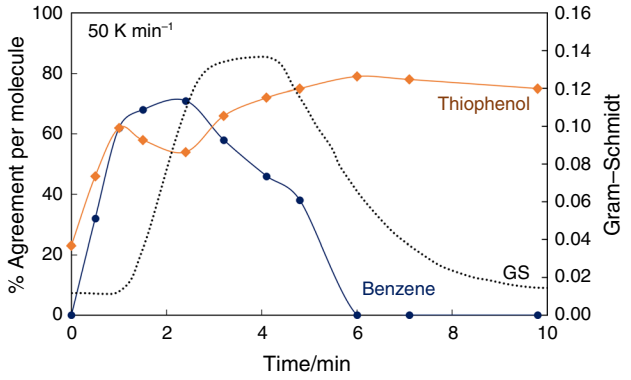

Fig. 8 TGA–FTIR agreement percentage between the experimental spectra of PPS thermal decomposition gases at 50 K min^{-1} under nitrogen, and the reference spectra of benzene and thiophenol. The time boundaries of the degradation process are deduced from the Gram–Schmidt signal

referenced infrared spectrum of given molecules has been verified. As mentioned in the introduction, PPS essentially decomposes by depolymerization which induces the formation of thiophenol or by random chain–scission which generates benzenic products [27, 28]. Therefore, the experimental spectra have been confronted with those of benzene and thiophenol.

An acceptable coincidence between the experimental data and the referenced spectra of both products is noticed at the early stages of the decomposition, and when the decomposition reaches its maximum rate. This is consistent with the expected competition between depolymerization and random chain-scission. The agreement percentage remains relatively constant along the whole process for thiophenol but decreases progressively for benzene which may suggest that depolymerization is the predominant mechanism of degradation. At the end of decomposition, the percentage of agreement drops to zero in the case of benzene but this is probably linked to the total absorbance being too weak for a correct estimation of coincidence between spectra. More likely, there is a coexistence of depolymerization and random chain-scission during the whole PPS thermal degradation, the depolymerization being slightly predominant.

In Fig. 9 are presented the results obtained from TGA–FTIR investigations on CF/PPS at 100 K min^{-1} (Fig. 9a) and 300 K min^{-1} (Fig. 9b). The choice of these heating rates has been done according to two criteria. As mentioned above, the total absorbance must be high enough to allow a proper estimation of the agreement percentage between experimental and reference spectra. Unfortunately, below 100 K min^{-1}, the allure of the Gram–Schmidt signal was too chaotic for a proper interpretation, even if the percentages of agreement were seemingly leading to the same conclusion than Fig. 8 i.e., the coexistence of random chain-scission and depolymerization. Furthermore, we decided to

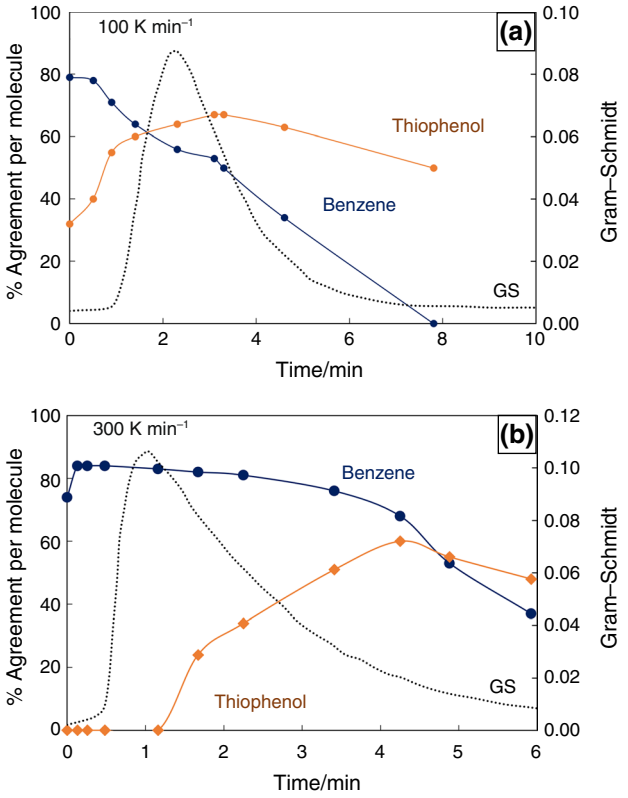

Fig. 9 TGA–FTIR agreement percentage between the experimental spectra of CF/PPS thermal decomposition gases at 100 and 300 K min^{-1} under nitrogen, and the reference spectra of benzene and thiophenol. The time boundaries of the degradation process are deduced from the Gram–Schmidt signal

exclude analyses performed above 300 K min^{-1}, because of the shift of TGA signature toward lower temperatures, which causes were not clearly identified. In other terms, we restricted the analysis to the case for which the increase in the heating rate induces the shift of degradation to higher temperatures.

Assuming the degradation process to be invariant of the heating rate, and considering that the carbon fibers do not undergo thermal decomposition within the temperature range scanned by the TGA, one can expect the decomposition products of CF/PPS to be the same than those of PPS, independently on the heating rate. One might even anticipate the percentage of agreement to remain consistent with the Gram–Schmidt profile. However, the obtained results did not match these hypotheses. At the maximum of the Gram–Schmidt signal, we find similar agreement between benzene and thiophenol when the TGA is performed at 100 K min^{-1}, but this agreement evolves to be largely in favor of benzene when the TGA is performed at 300 K min^{-1}. Moreover, it remains continuously higher along the whole degradation. This may indicate that the products from random chain–scission become predominant

at highest rates. Such interpretation is consistent with the findings of Perng [27] who reported that the depolymerization dominated in lower temperature pyrolysis while the main chain random scission dominated in higher temperature pyrolysis. Indeed, the increase of the heating rate induces the shift of the thermal decomposition to higher temperatures. Perng also reported that the chain transfer of carbonization gradually dominated at the higher pyrolysis temperature to form the high char yield of solid residue [27], which is consistent with our observation that the char amount increases with the heating rate. Thus, the degradation mechanisms could differ depending on the heating rate. Such influence of the heating rate on the decomposition mechanism was previously reported by other authors, working on different systems. Li et al. [51], studying algal waste, showed that fast pyrolysis produces about 50% more carbon dioxide than slow pyrolysis. These findings agree with those described by Efika et al. [52] on waste wood pellets, who reported, from investigations up to 350 K min^{-1}, a modification of the solid/liquid/gas product ratio with the increase in heating rate. Regarding PPS and CF/PPS, the evolution of the decomposition product ratio could be associated with a dominant process of degradation, i.e., the random chain–scission, progressively replacing the coexistence of the two main decomposition mechanisms when the heating rate increases.

Conclusions

Polymer matrix composites, which popularity continuously increases in the aeronautics field, face concerns regarding their structural integrity over fire. The safety requirements behind the aeronautical certifications push for improving the amount of knowledge about the mechanisms occurring during fast pyrolysis, since fire typically leads to a fast increase in temperature at the surface of the composite exposed to the flame, in the order of 400 K min^{-1}. From TGA data recorded at rates ranging from 5 to 500 K min^{-1}, this study addresses the question of the consistency of the interpretations based on experiments performed at conventional and high rates, respectively.

Firstly, it is showed that the calibration performed at 20 K min^{-1} is applicable to high-rate analyses. Although the post-calibration tests carried on a nickel standard have revealed a slight disagreement between the corrected and observed Curie transitions for rates above 50 K min^{-1}, the resulting impact on the measurement is still moderate as it never exceeds 10 °C and can be systematically corrected.

Then, it is highlighted that the perception of the polymer decomposition is modified by the experimental conditions, due to the impact of both the heating rate and the sample mass on the signature of decomposition. In particular, the investigations regarding the thermal decomposition of polymeric systems have evidenced a complex heating rate dependence of the TGA response, i.e., non-monotonic and irregular variations of the characteristic temperatures of decomposition as a function of the heating rate.

Eventually, high-rate measurements have been carried on PPS and CF/PPS. It has been observed that the amount of residue increases with the heating rate. Interestingly, this behavior is not a characteristic of all «char–forming» materials. Indeed, for PEEK and PEKK compounds, the amount of «char» decreases when increasing the heating rate. To preserve the structural stability of a component, the mass loss must be limited. Thus, CF/PPS stands out among polymer matrix composites targeting aeronautic applications by exhibiting an interesting thermal stability feature.

Possible mechanistic causes behind this behavior have been explored by TGA–FTIR investigations. At high rates, the decomposition gazes differ in composition. The expected formation of thiophenol, characteristic of depolymerization, is contradicted by infrared spectra, indicating instead that the process of random chain–scission, at the origin of the formation of benzene is predominant. Therefore, this study points out that the thermal decomposition at high rates has its proper specificities and deserves further investigations.

Supplementary Information The online version contains supplementary material available at https://doi.org/10.1007/s10973-024-13208-2.

Author contributions ND, BV, ED: Conceptualization, Supervision; ND: Methodology, Writing–original draft preparation; YC, AB: Formal analysis and investigation; ND, YC, ED, BV: Writing–review and editing; BV: Funding acquisition; ED, BV: Resources

References

1. Hshieh F-Y, Beeson HD. Flammability testing of flame-retarded epoxy composites and phenolic composites. Fire Mater. 1997;21:41–9. https://doi.org/10.1002/(SICI)1099-1018(199701)21:1%3c41::AID-FAM595%3e3.0.CO;2-G.
2. Dodds N, Gibson AG, Dewhurst D, Davies JM. Fire behaviour of composite laminates. Compos Part A: Appl Sci Manuf. 2000;31:689–702. https://doi.org/10.1016/S1359-835X(00)00015-4.
3. Gibson AG. The integrity of polymer composites during and after fire. J Compos Mater. 2004;38:1283–308. https://doi.org/10.1177/0021998304042733.
4. Lattimer BY, Ouellette J. Properties of composite materials for thermal analysis involving fires. Compos Part A: Appl Sci Manuf. 2006;37:1068–81. https://doi.org/10.1016/j.compositesa.2005.01.029.
5. Michael Davies J, Wang Y, Wong P. Polymer composites in fire. Compos Part A: Appl Sci Manuf. 2006;37:1131–41. https://doi.org/10.1016/j.compositesa.2005.05.032.
6. La Delfa G, Luinge J, Gibson AG. Next generation composite aircraft fuselage materials under post-crash fire conditions. In: Pantelakis S, Rodopoulos C (Eds.). Engineering against Fracture: Proceedings of the 1st Conference. Springer Netherlands, Dordrecht. 2009. pp.169–81

7. Mouritz AP, Feih S, Kandare E, Mathys Z, Gibson AG, Des Jardin PE, Case SW, Lattimer BY. Review of fire structural modelling of polymer composites. Compos Part A: Appl Sci Manuf. 2009;40:1800–14. https://doi.org/10.1016/j.compositesa.2009.09.001.
8. Perret B, Schartel B, Stöß K, Ciesielski M, Diederichs J, Döring M, Krämer J, Altstädt V. Novel DOPO-based flame retardants in high-performance carbon fibre epoxy composites for aviation. Eur Polym J. 2011;47:1081–9. https://doi.org/10.1016/j.eurpolymj.2011.02.008.
9. Ma CC, Hsia HC, Liu WL, Hu JT. Studies on thermogravimetric properties of polyphenylene sulfide and polyetherether ketone resins and composites. J Thermoplast Compos Mater. 1988;1(1):39–49. https://doi.org/10.1177/089270578800100010.
10. Arvind A, Sanjay A. An experimental and theoretical investigation into burning characteristics of PS-glass fiber composites. In: 8th AIAA/ASME Joint Thermophysics and Heat Transfer Conference. American Institute of Aeronautics and Astronautics, St. Louis Michigan. 2002
11. Mouritz AP, Gibson AG. Fire Properties of Polymer Composite Materials. Netherlands: Springer Science and Business Media; 2007.
12. Patel P, Hull TR, Lyon RE, Stoliarov SI, Walters RN, Crowley S, Safronava N. Investigation of the thermal decomposition and flammability of PEEK and its carbon and glass–fibre composites. Polym Degrad Stabil. 2011;96:12–22. https://doi.org/10.1016/j.polymdegradstab.2010.11.009.
13. Vieille B, Lefebvre C, Coppalle A. Post fire behavior of carbon fibers Polyphenylene Sulfide-and epoxy-based laminates for aeronautical applications: a comparative study. Mater Des. 2014;63:56–68. https://doi.org/10.1016/j.matdes.2014.05.046.
14. Vieille B, Coppalle A, Keller C, Garda M, Viel Q, Dargent E. Correlation between post fire behavior and microstructure degradation of aeronautical polymer composites. Mater Des. 2015;74:76–85. https://doi.org/10.1016/j.matdes.2015.03.002.
15. Zhang J, Delichatsios MA, Fateh T, Suzanne M, Ukleja S. Characterization of flammability and fire resistance of carbon fibre reinforced thermoset and thermoplastic composite materials. J Loss Prev Process Ind. 2017;50:275–82. https://doi.org/10.1016/j.jlp.2017.10.004.
16. Schuhler E, Coppalle A, Vieille B, Yon J, Carpier Y. Behaviour of aeronautical polymer composite to flame: a comparative study of thermoset–and thermoplastic–based laminate. Polym Degrad Stabil. 2018;152:105–15. https://doi.org/10.1016/j.polymdegradstab.2018.04.004.
17. Vieille B, Casado VM, Bouvet C. About the impact behavior of woven-ply carbon fiber-reinforced thermoplastic–and thermosetting–composites: a comparative study. Compos Struct. 2013;101:9–21. https://doi.org/10.1016/j.compstruct.2013.01.025.
18. Cao FC, Ma XY, Zhou HL, Tang Y, Dong XL, Huang AC. Enhanced suppression of metal combustion processes using a compound expansible graphite extinguishing agent: experimental study and mechanistic insights. J Loss Prev Process Ind. 2023;85:105154. https://doi.org/10.1016/j.jlp.2023.105154.
19. Bourbigot S, Delobel R, Duquesne S. Comportement au feu des composites. Techniques de l'ingénieur. 2006. AM5330. https://doi.org/10.51257/a-v1-am5330
20. Guillaume E. Modélisation de la décomposition thermique des matériaux en cas d'incendie. Techniques de l'ingénieur. 2015. 2066. https://doi.org/10.51257/a-v1-se2066
21. Chetehouna K, Grange N, Gascoin N, Lemée L, Reynaud I, Senave S. Release and flammability evaluation of pyrolysis gases from carbon-based composite materials undergoing fire conditions. J Anal Appl Pyrolysis. 2018;134:136–42. https://doi.org/10.1016/j.jaap.2018.06.001.
22. Feih S, Mouritz AP. Tensile properties of carbon fibres and carbon fibre–polymer composites in fire. Compos Part A: Appl Sci Manuf. 2012;43:765–72. https://doi.org/10.1016/j.compositesa.2011.06.016.
23. Beyler CL, Hirschler MM. Thermal decomposition of polymers. In: DiNenno PJ, Drysale D, Beyler CL, Douglas Walton W, Custer RLP, Hall JR, Watts JM, editors. SFPE Handbook of Fire Protection Engineering, vol. 7. 3rd ed. Quincy: National Fire Protection Association Inc; 2002. p. 110–31.
24. Liu YC, Jiang JC, Huang AC. Experimental study on extinguishing oil fire by water mist with polymer composite additives. J Therm Anal Calorim. 2023;148(11):4811–22. https://doi.org/10.1007/s10973-022-11645-5.
25. Montaudo G, Puglisi C, Samperi F. Primary thermal degradation processes occurring in poly (phenylenesulfide) investigated by direct pyrolysis–mass spectrometry. J Polym Sci Part A: Polym Chem. 1994;32(10):1807–15. https://doi.org/10.1002/pola.1994.080321002.
26. Budgell DR, Day M, Cooney JD. Thermal degradation of poly (phenylene sulfide) as monitored by pyrolysis—GC/MS. Polym Degrad Stabil. 1994;43:109–15. https://doi.org/10.1016/0141-3910(94)90232-1.
27. Perng LH. Thermal decomposition characteristics of poly (phenylene sulfide) by stepwise Py–GC/MS and TG/MS techniques. Polym Degrad Stabil. 2000;69:323–32. https://doi.org/10.1016/S0141-3910(00)00077-X.
28. Peters OA, Still RH. The thermal degradation of poly (phenylene sulphide)—part 1. Polym Degrad Stabil. 1993;42:41–8. https://doi.org/10.1016/0141-3910(93)90023-C.
29. Di HW, Fan C, He H, Zhang N, Dong JL, Wang YT. A novel EVA-based composite via ceramization toward excellent flame retardance performance and high-temperature resistance. J Therm Anal Calorim. 2023;148(21):11717–26. https://doi.org/10.1007/s10973-023-12524-3.
30. Feng J, Hao J, Du J, Yang R. Using TGA/FTIR TGA/MS and cone calorimetry to understand thermal degradation and flame retardancy mechanism of polycarbonate filled with solid bisphenol A bis(diphenyl phosphate) and montmorillonite. Polym Degrad Stabil. 2012;97:1506–14. https://doi.org/10.1016/j.polymdegradstab.2012.01.011.
31. Xu J, Liu C, Qu H, Ma H, Jiao Y, Xie J. Investigation on the thermal degradation of flexible poly(vinyl chloride) filled with ferrites as flame retardant and smoke suppressant using TGA–FTIR and TGA–MS. Polym Degrad Stabil. 2013;98:605–14. https://doi.org/10.1016/j.polymdegradstab.2013.04.016.
32. Erickson KL. Thermal decomposition mechanisms common to polyurethane, epoxy, poly (diallyl phthalate), polycarbonate and poly (phenylene sulfide). J Therm Anal Calorim. 2007;89:427–40. https://doi.org/10.1007/s10973-006-8218-6.
33. Carpier Y, Vieille B, Delpouve N, Dargent E. Isothermal and anisothermal decomposition of carbon fibres polyphenylene sulfide composites for fire behavior analysis. Fire Safety J. 2019;109:102868. https://doi.org/10.1016/j.firesaf.2019.102868.
34. Vanden Poel G, Mathot VBF. High-speed/high performance differential scanning calorimetry (HPer DSC): temperature calibration in the heating and cooling mode and minimization of thermal lag. Thermochim Acta. 2006;446:41–54. https://doi.org/10.1016/j.tca.2006.02.022.
35. Vieille B, Ernault E, Delpouve N, Pujols Gonzalez J-D, Esposito A, Dargent E, Le Pluart L, Delbreilh L. On the improvement of thermo-mechanical behavior of carbon/polyphenylene sulfide laminated composites upon annealing at high temperature. Compos Part B-Eng. 2021;216:108858. https://doi.org/10.1016/j.compositesb.2021.108858.
36. TGA temperature calibration using curie temperature standards. TA Instruments® Application Note TA 427

37. Moneta M, Wasiak M, Sovak P. Temperature dependence of structural and magnetic transformations in finemet-type amorphous alloys with Fe substituted for La. J Therm Anal Calorim. 2023;148(4):1577–80. https://doi.org/10.1007/s10973-022-11675-z.
38. Norem SD, O'Neill MJ, Gray AP. The use of magnetic transitions in temperature calibration and performance evaluation of thermogravimetric systems. Thermochimica Acta. 1970;1(1):29–38. https://doi.org/10.1016/0040-6031(70)85026-2.
39. Hasier J, Riolo MA, Nash P. Curie temperature determination via thermogravimetric and continuous wavelet transformation analysis. EPJ Techn Instrum. 2017;4:5. https://doi.org/10.1140/epjti/s40485-017-0040-y.
40. Levchik S, Wilkie CA. Char formation. In: Grand AF, Wilkie CA, editors. Fire Retardancy of Polymeric Materials. New York: Marcel Dekker Inc; 2000. p. 171–216.
41. Mouritz AP, Gibson AG. Fire properties of polymer composite materials. Dordrecht: Springer; 2006.
42. Price D, Anthony G, Carty P. Introduction: polymer combustion, condensed phase pyrolysis and smoke formation. In: Horrocks AR, Price D, editors. Fire Retardant Materials. Cambridge: Woodhead Publishing Ltd; 2002. p. 1–30.
43. Pering GA, Farrell PV, Springer GS. Degradation of tensile and shear properties of composites exposed to fire or high temperature. J Compos Mater. 1989;14:54–66.
44. Parker JA, Kourtides DA. New fireworthy composites for use in transportation vehicles. J Fire Sci. 1983;1:432–58. https://doi.org/10.1177/073490418300100060.
45. Yao F, Zheng J, Qi M, Wang W, Qi Z. The thermal decomposition kinetics of poly (ether–ether–ketone) (PEEK) and its carbon fiber composite. Thermochim Acta. 1991;183:91–7. https://doi.org/10.1016/0040-6031(91)80448-R.
46. Vieille B, Coppalle A, Le Pluart L, Schuhler E, Chaudhary A, Rijal B, Alia A, Delpouve N, Bourdet A. Influence of a flame-retardant on the fire–behaviour and the residual mechanical properties of C/PEKK composite laminates exposed to a kerosene flame. Compos Part A: Appl Sci Manuf. 2022;152:106720. https://doi.org/10.1016/j.compositesa.2021.106720.
47. Vieille B, Coppalle A, Schuhler E, Chaudhary A, Alia A, Delpouve N, Bourdet A. Influence of kerosene flame on fire-behaviour and mechanical properties of hybrid carbon glass fibers reinforced PEEK composite laminates. Compos Struct. 2022;279:114786. https://doi.org/10.1016/j.compstruct.2021.114786.
48. Anderson JJ. Retention of flame properties of rigid polyurethane foams. Ind Eng Chem Prod Res Dev. 1963;2:260–3. https://doi.org/10.1021/i360008a003.
49. Toor SS, Rosendahl L, Sintamarean I. Recipe-based co–HTL of biomass and organic waste. In: Rosendahl L, editor. Direct thermochemical liquefaction for energy applications. Amsterdam: Woodhead Publishing Elsevier; 2018. p. 169–89.
50. Shelden B, Erickson, KL, Dodd, AB (2013) Numerical Simulation of Decomposition and Combustion of an Epoxy-Carbon-Fiber Composite. Conference Interflam 2013, 13th International Conference and Exhibition on Fire Science and Engineering. Royal Holloway College, Nr Windsor, UK. pp.24–26. https://www.osti.gov/servlets/purl/1661391
51. Li M, Zhang YS, Cheng S, Qu B, Li A, Meng F, Ji G. The impact of heating rate on the decomposition kinetics and product distribution of algal waste pyrolysis with in–situ weight measurement. Chem Eng J. 2023;457:141368. https://doi.org/10.1016/j.cej.2023.141368.
52. Efika CE, Onwudili JA, Williams PT. Influence of heating rates on the products of high–temperature pyrolysis of waste wood pellets and biomass model compounds. Waste Manage. 2018;76:497–506. https://doi.org/10.1016/j.wasman.2018.03.021.